

Quantifying stochasticity in the dynamics of delay-coupled semiconductor lasers via forbidden patterns

Jordi Tiana-Alsina, Javier M. Buldú, M. C. Torrent and Jordi García-Ojalvo

Phil. Trans. R. Soc. A 2010 **368**, 367-377

doi: 10.1098/rsta.2009.0241

References

[This article cites 19 articles](#)

<http://rsta.royalsocietypublishing.org/content/368/1911/367.full.html#ref-list-1>

Rapid response

[Respond to this article](#)

<http://rsta.royalsocietypublishing.org/letters/submit/roypta;368/1911/367>

Subject collections

Articles on similar topics can be found in the following collections

[complexity](#) (15 articles)

Email alerting service

Receive free email alerts when new articles cite this article - sign up in the box at the top right-hand corner of the article or click [here](#)

To subscribe to *Phil. Trans. R. Soc. A* go to:

<http://rsta.royalsocietypublishing.org/subscriptions>

Quantifying stochasticity in the dynamics of delay-coupled semiconductor lasers via forbidden patterns

BY JORDI TIANA-ALSINA¹, JAVIER M. BULDÚ², M. C. TORRENT¹
AND JORDI GARCÍA-OJALVO^{1,*}

¹*Departament de Física i Enginyeria Nuclear, Universitat Politècnica de Catalunya, Colom 11, 08222 Terrassa, Barcelona, Spain*

²*Complex Systems Group, Department of Signal Theory and Communications, Universidad Rey Juan Carlos, Camino del Molino s/n, 28943 Fuenlabrada, Madrid, Spain*

We quantify the level of stochasticity in the dynamics of two mutually coupled semiconductor lasers. Specifically, we concentrate on a regime in which the lasers synchronize their dynamics with a non-zero lag time, and the leader and laggard roles alternate irregularly between the lasers. We analyse this switching dynamics in terms of the number of forbidden patterns of the alternate time series. The results reveal that the system operates in a stochastic regime, with the level of stochasticity decreasing as the lasers are pumped further away from their lasing threshold. This behaviour is similar to that exhibited by a single semiconductor laser subject to external optical feedback, as its dynamics shifts from the regime of low-frequency fluctuations to coherence collapse.

Keywords: delay-coupled oscillators; forbidden patterns; noise; semiconductor laser dynamics; low-frequency fluctuations

1. Introduction

When dynamical systems interact, they do so via signals that travel at finite speeds, thus leading to coupling delays (Herrero *et al.* 2000; Takamatsu *et al.* 2000). If these delay times are of the order of, or larger than, the characteristic time scales of individual oscillators, simultaneous synchronization between the interacting systems usually cannot occur (Uchida *et al.* 2005). In the simplest situation of a pair of oscillators coupled unidirectionally, the emitter advances the receiver by a time equal to the coupling delay time. When coupling is bidirectional, the situation is not so clear. Symmetry considerations would lead one to expect that the oscillators should synchronize with zero lag, but that simultaneous state is frequently unstable, leading to a spontaneous symmetry breaking of the collective dynamics.

Such symmetry breaking was first reported experimentally by Heil *et al.* (2001) in a system of two semiconductor lasers coupled to each other by the mutual injection of their emitted light. In that case, coupling destabilizes the laser

*Author for correspondence (jordi.g.ojalvo@upc.edu).

One contribution of 13 to a Theme Issue ‘Delayed complex systems’.

emission, leading (for distances between the lasers of centimetres and higher) to sudden and short-lived power dropouts at irregular times. When the lasers have sufficiently different frequencies (more than 1 GHz apart), the temporal organization of the synchronized state is well defined: the laser with the largest frequency always drops out in power first. For zero-frequency detuning, however, the leader and laggard roles alternate irregularly in time between the two lasers. The question then arises, of whether this irregular dynamics is chaotic or is dominated by noise. A similar issue exists in the case of a semiconductor laser with optical feedback (Ohtsubo 2002), which for moderate feedback levels exhibits a dynamic behaviour similar to the one described above, consisting of sudden dropouts in the emitted light intensity occurring at irregular times and called low-frequency fluctuations (LFFs), since their time scale (approx. microseconds) is much longer than the intrinsic time scale of the device (approx. picoseconds).

Two different explanations were initially proposed for the LFF phenomenon. In the first, the dropouts were stochastic events caused by spontaneous emission fluctuations (Henry & Kazarinov 1986). In the second, the LFFs were considered to be an instance of chaotic dynamics (Mork *et al.* 1992) and intermittent behaviour (Sacher *et al.* 1989). The second view was substantiated soon afterwards by Sano (1994), through an analysis of the LFF trajectories in phase space and their interaction with the many (unstable) fixed points of the delay–differential equation model that represents the dynamics of the system. A more detailed experimental and numerical investigation of the system (Hohl *et al.* 1995; Lam *et al.* 2003) revealed that both deterministic and stochastic mechanisms are necessary to explain the existence of LFFs, with noise being more important close to the lasing threshold and chaos prevailing far from threshold, on the way to the fully developed chaotic regime known as coherence collapse (Ohtsubo 2002).

In this paper, we address the issue of how stochastic the dynamics of two mutually coupled semiconductor lasers is, in the leader–laggard dynamical regime described above, which is analogous to the LFF regime exhibited by a single semiconductor laser with optical feedback. We use an approach recently introduced by Amigó *et al.* (2006), consisting in analysing the set of all order patterns of a time series (defined as order sequences of subsets of elements of the time series). A random series of infinite length contains all possible order patterns with probability one, whereas in a chaotic time series certain order sequences will never occur owing to the structure of the phase space in which they evolve. Identifying the existence of such forbidden patterns in our time series should tell us whether they have an underlying deterministic behaviour. This technique has been used to characterize the level (or lack) of stochasticity in logistic maps (Amigó *et al.* 2006), shift systems (Amigó *et al.* 2008), and financial time series (Zanin 2008; Zunino *et al.* 2009). Here we report on what is, as far as we know, the first application of this method to experimentally generated time series. In our case, as shown below, the leader–laggard dynamics provides us with a natural way of generating a symbolic time series and thus no order patterns must be extracted from the experimental measurements. Furthermore, owing to the high dimensionality of the dynamics of semiconductor lasers subject to delayed optical injection (Ahlers *et al.* 1998), the number of forbidden sequences eventually drops to zero for sufficiently long time series, and hence we quantify the level of stochasticity in terms of how fast the number of forbidden patterns decays

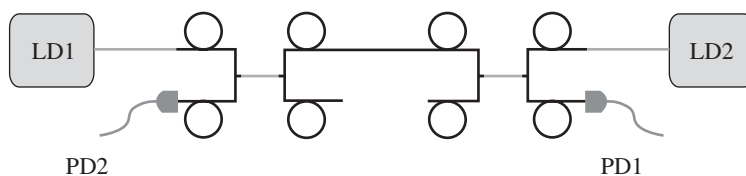


Figure 1. Experimental setup. Two semiconductor lasers (LD1 and LD2) inject their emitted light into each other via an optical fibre. PD1 and PD2 are photodetectors.

with length. Our results show that, similar to the case of a single semiconductor laser subject to optical feedback, the dynamics is more stochastic the closer the lasers are to their emission threshold. We organize the paper as follows. The next section contains a description of the experimental setup. Section 3 details the experimental results obtained, and §4 presents numerical results that contextualize the experimental observations presented earlier.

2. Experimental setup

Figure 1 shows a schematic diagram of the setup used in the experiments reported below. Two semiconductor lasers (Mitsubishi ML925B45F) at a distance of 6 m from each other are bidirectionally coupled via an optical fibre. Coupling is achieved by means of an optical coupler with a 50/50 coupling ratio (10202A-50-FC). The lasers operate at a nominal wavelength $\lambda_n = 1550$ nm and a nominal power of 6 mW. The temperature and pump current of the lasers are controlled with an accuracy of 0.01°C and 0.01 mA, respectively, and are adjusted such that their optical frequencies when isolated are as similar as possible to each other. For temperatures $T_{\text{LD1}} = 10.97^\circ\text{C}$ and $T_{\text{LD2}} = 20.75^\circ\text{C}$, the threshold currents of the solitary lasers are, respectively, $I_{\text{LD1}}^{\text{th}} = 11.10$ mA and $I_{\text{LD2}}^{\text{th}} = 11.63$ mA. The laser intensities are captured by high-speed fibre photodetectors with 2 GHz bandwidth (DET01CFC). The received signals are amplified, using a 2 GHz femto high-speed amplifier, and sent to a 1 GHz oscilloscope (Agilent DS06104A). Note that owing to the limited bandwidth of the detectors, we are only able to monitor the slow dynamics of the system, which is enough for our study.

This setup allows us to control the leader–laggard dynamics of the system. In particular, the relative wavelengths of the lasers in isolation determine which laser leads the dynamics. The wavelengths can be tuned by adjusting the lasers’ pump current. As mentioned above, the laser detuned to higher frequencies always takes the leader role. We now show that, for a large range of parameters, the detuning can be made small enough so that no clear leader exists.

3. Experimental results

For the experimental conditions given above, the two otherwise stable semiconductor lasers start pulsing in the form of synchronized power dropouts. The dropouts do not occur simultaneously, but are separated by a time of approximately 30 ns, corresponding to the time taken by light to travel between the two lasers. When the pump currents of the lasers are adequately fine-tuned,

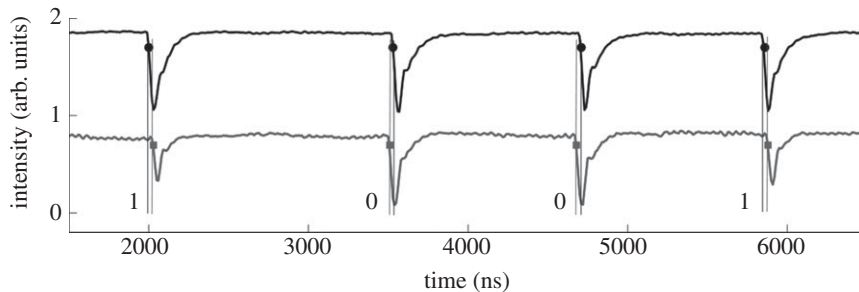


Figure 2. Experimental output intensities of the two coupled lasers. Laser LD1 is shown in the top trace and laser LD2 in the bottom trace. The pump current of LD1 is 13.38 mA and that of LD2 is 12.25 mA. The time trace of LD1 has been shifted upwards for clarity. The symbols indicate the times at which the dropouts occur. Vertical lines are added at the dropout locations to allow comparison between the dropout times of the two lasers. The numbers at the bottom of the vertical lines indicate the binary value associated with the ordering of the dropouts between the two lasers.

the frequency detuning between them is approximately zero and the leading role of the dynamics alternated between the two lasers, as explained above and shown in figure 2. The plot portrays a sample pair of simultaneously measured time traces, with the dropouts of each laser identified by the time instant at which the intensity drops below a certain threshold, chosen in order to optimize the detection of the dropouts, while being consistent between the two lasers. In the particular sample shown in the figure, laser LD1 (top trace) leads the dynamics in the first and fourth dropouts, while laser LD2 (bottom trace) is the leader for the second and third dropouts. A statistical analysis of the data indicates that the leader and laggard roles switch irregularly in time, and that the ordering of each leader–laggard event is independent of all other previous events.

In order to quantify how the leader and laggard roles are distributed between the two lasers, we measured the time interval between each pair of synchronized dropouts. Figure 3 shows histograms of the inter-dropout intervals for different values of the pump currents of laser LD1, having fixed the value of LD2's pump current. The figure shows that, as laser LD1 is pumped at smaller current levels, the leader role shifts from LD2 (*a*) to LD1 (*b*). These situations correspond to the corresponding leading laser having a larger frequency. For an intermediate value of LD1's pump current (*c*), the frequencies of the two lasers can be made to coincide. In that case, the leader role is equally distributed among the two lasers.

Our goal is to determine the level of stochasticity of the irregular leader–laggard alternating dynamics shown in figures 2 and 3*c*. To that end, we use a recently introduced technique based on forbidden patterns (Amigó *et al.* 2006). In its original implementation, this technique used ordinal patterns in order to convert a continuous into a discrete time series (Zunino *et al.* 2009). In our case, however, there is a natural way of converting the analogue character of the laser intensities into a discrete time series. The method is illustrated in figure 2. Simply put, we assign one of the two binary values to each pair of synchronized dropouts, depending on which laser drops in intensity first. If the dropout of LD1 occurs earlier than that of LD2, we assign a '1', and in the opposite case we assign a '0'. In this way, we convert the two analogue time series corresponding to the laser

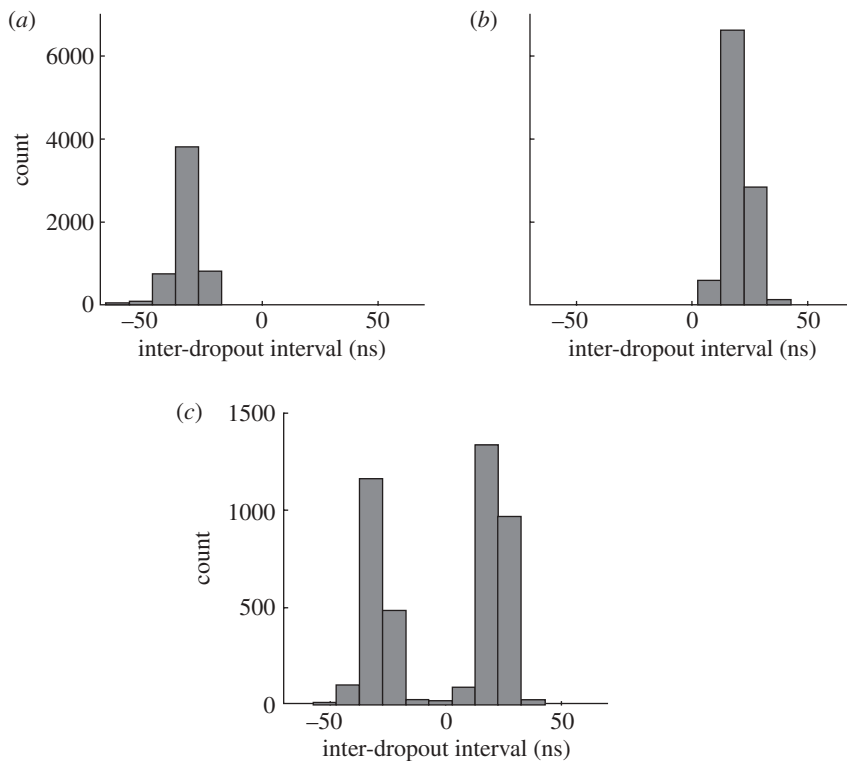


Figure 3. Histograms of time interval between dropouts for two coupled lasers for varying pumping of laser LD1: (a) $I_{LD1} = 13.84$ mA, (b) $I_{LD1} = 12.38$ mA and (c) $I_{LD1} = 13.38$ mA. The pump current for LD2 is $I_{LD2} = 12.25$ mA in all three cases.

outputs to a single binary time series for which we can characterize the statistics of patterns of a certain bit length. By way of example, and additionally as a way of quantifying the leader–laggard transition partially shown in figure 3, we show in figure 4 the number of forbidden patterns of length equal to 8 bits versus the pump current of LD1, keeping LD2’s pump current constant. The calculation is made by scanning the binarized time series with an 8 bit long box, and moving 1 bit at every step. Once all occurring patterns are identified, we compare the list of those patterns with the list of all possible patterns, which equals 256 for a box of length 8. Those patterns out of the 256 that do not appear a single time are labelled as forbidden. For a long enough bit sequence, the existence of forbidden patterns should indicate the deterministic character of the underlying continuous dynamics. Figure 4 shows the expected result that, when one of the lasers leads the dynamics, most of the time series consists of either ‘0’s or ‘1’s, and thus a large number of 8 bit forbidden patterns exists, the number being close to 256. On the other hand, in the situation of a perfect leader/laggard alternance, the number of forbidden patterns decreases rather sharply to zero, even when the length of the time series is finite. Incidentally, the range of pump current values for which the time series is stochastic is rather large, of the order of several tenths of a milliamper.

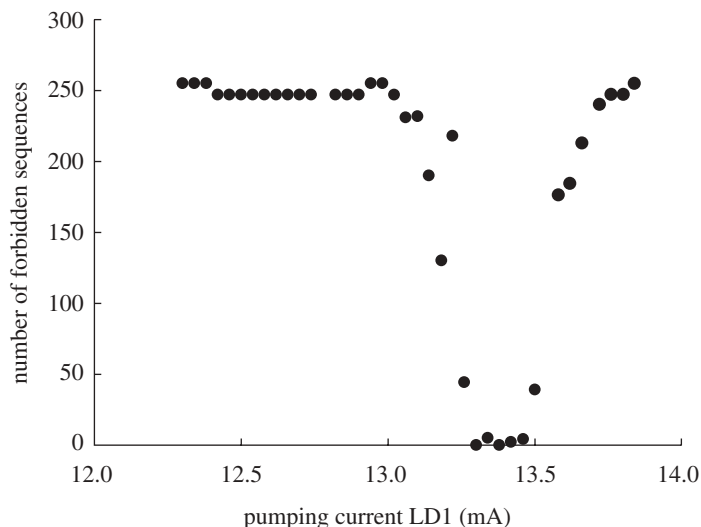


Figure 4. Number of forbidden patterns of length equal to 8 bits for increasing pump current of laser LD1. The pump current of LD2 is fixed to $I_{LD2} = 12.25$ mA.

In the remainder of the paper, we concentrate on the situation in which the leader and laggard roles are equally distributed among the two lasers (figure 3c). The fact that the number of forbidden patterns is zero in that case, as shown in the preceding figure, does not necessarily mean that the time series is stochastic, since semiconductor lasers with delay are known to be highly dimensional chaotic systems (Ahlers *et al.* 1998). Chaotic systems should exhibit a non-zero number of forbidden patterns (Amigó *et al.* 2006), but if the chaotic attractor is highly dimensional and the pattern length is too small, they would not appear distinguishable from a stochastic time series. Increasing the pattern length is usually unfeasible, since it would require the length of the measured time series to be increased unrealistically (Amigó *et al.* 2007).

It is known, for instance, that, in diode lasers with optical feedback, stochasticity is important near threshold (Hohl *et al.* 1995; Lam *et al.* 2003), while deterministic (i.e. chaotic) mechanisms play a relevant role further away from threshold (Fischer *et al.* 1996). Given the similarities between the dynamics of a semiconductor laser with optical feedback and two mutually coupled semiconductor lasers, we can expect a similar trend to occur in the latter system. In order to see whether systematic differences between the levels of stochasticity exist in our system as we approach the lasing threshold, we plot in figure 5 the number of forbidden patterns versus the total series length for three different values of the pump current of LD1, while fixing the pump current of LD2 to a value such that the leader/laggard alternance is split 50/50 among the two lasers in each case. The first feature shown in this figure is that, as the length of the time series being analysed increases, the number of forbidden patterns decreases in all cases, since it becomes easier to detect rare patterns (Amigó *et al.* 2007). The rate at which the number of forbidden patterns decreases to zero is, however, different for different pump strengths: for smaller pump currents,

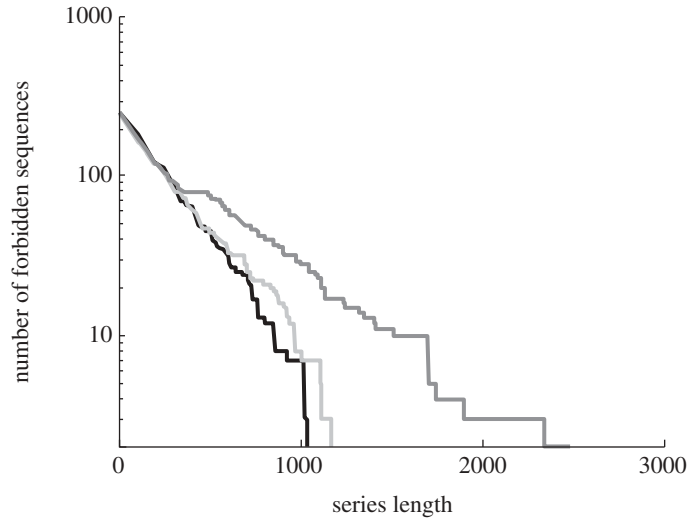


Figure 5. Number of forbidden patterns for increasing length of the time series, and for three different values of the pump current of LD1: 12.00 mA (black), 12.25 mA (light grey) and 12.85 mA (dark grey). The pump current of LD2 is for each case: 12.62 (black), 13.38 (light grey) and 12.76 mA (dark grey).

i.e. closer to threshold (black line in figure 5), the decay to zero is very fast, indicating that the process is strongly stochastic. As the pump current increases, the decay becomes clearly slower, which indicates that the level of stochasticity in the dynamics monotonically decreases as LD1 is pumped further away from its threshold. Thus, these experimental results confirm the expectation that in mutually coupled semiconductor lasers, similar to the case of single semiconductor lasers with optical feedback, the dynamics is more stochastic closer to threshold, while further away from threshold noise plays a lesser role.

4. Numerical simulations

In the previous experimental study, the pump current of laser LD2 had to be tuned for each value of the pump current of LD1 so that 50/50 leader/laggard alternance was maintained as LD1 was pumped increasingly further away from its threshold. It could then be argued that the joint lasing threshold of the system was not being increased monotonically in figure 5. In order to confirm that indeed the stochasticity of the dynamics increases gradually as we approach threshold, we now perform numerical simulations of an ideal version of the system studied experimentally above. To that end, we use a generalized version of the Lang–Kobayashi model that reads (González *et al.* 2007):

$$\frac{dE_1}{dt} = \frac{1 + i\alpha}{2}(G_1 - \gamma_1)E_1(t) + \kappa_{21}e^{i(\Delta\omega t - \omega_2\tau_{21})}E_2(t - \tau_{21}) + \sqrt{2\beta N_1}\xi_1(t), \quad (4.1)$$

$$\frac{dE_2}{dt} = \frac{1 + i\alpha}{2}(G_2 - \gamma_2)E_2(t) + \kappa_{12}e^{i(\Delta\omega t - \omega_1\tau_{12})}E_1(t - \tau_{12}) + \sqrt{2\beta N_2}\xi_2(t) \quad (4.2)$$

Table 1. Laser parameters of the numerical model in the LFF regime.

symbol	parameter	value
$I_{1,2}^P$	pump current of LD1,2	$(1.02 \text{ to } 1.07) \times I_{\text{th}}$
τ_{12}	coupling time path 1 \rightarrow 2	3.4 ns
τ_{21}	coupling time path 2 \rightarrow 1	3.4 ns
κ_{12}	coupling strength path 1 \rightarrow 2	30 ns^{-1}
κ_{21}	coupling strength path 2 \rightarrow 1	30 ns^{-1}
γ_e	inverse carrier lifetime	$6.89 \times 10^{-4} \text{ ns}^{-1}$
γ	inverse photon lifetime	0.480 ps^{-1}
N_0	carrier number at transparency	1.25×10^8
N_{th}	carrier number at threshold	1.634×10^8
g	gain parameter	$1.25 \times 10^{-8} \text{ ps}^{-1}$
α	linewidth enhancement factor	3.5
β	noise intensity	$10^{-15} \text{ to } 10^{-11} \text{ ps}^{-2}$

and

$$\frac{dN_{1,2}}{dt} = C_b - \gamma_e N_{\text{th}} - G_{1,2} I_{1,2}(t). \quad (4.3)$$

Here $E_{1,2}(t)$ are the electric fields and $N_{1,2}$ the carrier numbers of lasers LD1 and LD2, respectively. The lasers' intensities are denoted by $I_{1,2}(t) = |E_{1,2}(t)|^2$, while $\omega_{1,2}$ represents the free-running optical frequencies of the two lasers. The detuning between the lasers is $\Delta\omega = \omega_1 - \omega_2$, which we have assumed for simplicity to be zero. The first term on the right-hand side of equations (4.1) and (4.2) corresponds to stimulated emission. The linewidth enhancement factor α is assumed to be the same for both lasers, $\gamma_{1,2}$ is the inverse photon lifetime and $G_{1,2} = g_{1,2}(N_{1,2} - N_{1,2}^0)$ is the gain (assumed linear), where $N_{1,2}^0$ denotes the carrier number at transparency and $g_{1,2}$ the differential gain (gain saturation is neglected because the lasers operate close to threshold). The second term in equations (4.1) and (4.2) is the coupling term, characterized by τ_{ij} (injection delay time) and κ_{ij} (injection coupling strength). Finally, the last term in those equations corresponds to the spontaneous emission noise, represented by a Gaussian white noise of zero mean, with a spontaneous emission rate β .

The carrier density equation, equation (4.3), contains three terms. The first term is the bias current (defined as $C_b = \gamma_e N_{\text{th}}(I_i^P/I_{\text{th}})$, where $N_{\text{th}} = \gamma_i/g + N_0$) corresponding to the pump current of each laser. The second and third terms are related to spontaneous and stimulated electron-hole recombinations, respectively. Table 1 lists the parameter values used in the numerical simulations described below. For these parameters, the coupled-laser system operates in the LFF regime.

We performed extensive numerical simulations of the model described above, in the case where the two lasers exhibit synchronous power dropouts. Since the model assumes no frequency detuning, the simulations produce naturally complete alternance between the leader and laggard roles for the two lasers. Under those conditions, we studied how the number of forbidden patterns varies as the pump currents of *both lasers* increase further away from threshold. The results

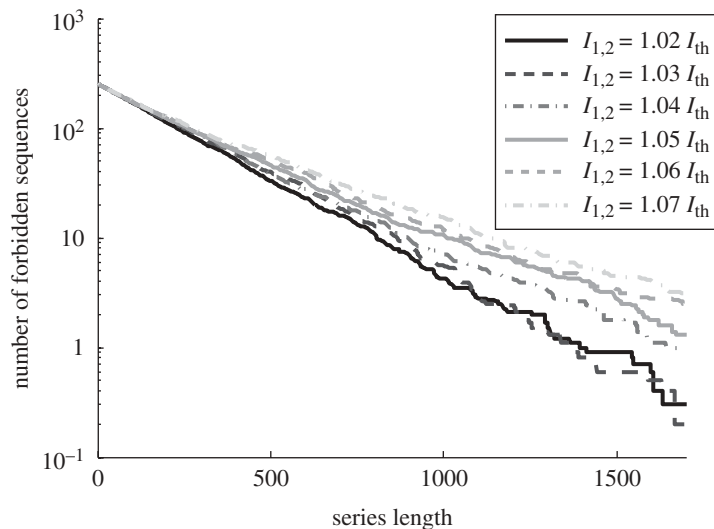


Figure 6. Number of forbidden sequences of the numerically simulated coupled time series for increasing length of the series and for different values of the pump currents (assumed equal for the two lasers).

are summarized in figure 6. As in the experimental results reported above, here the number of forbidden sequences decays to zero slower the further away the system is from threshold, indicating that the level of stochasticity is larger close to threshold and smaller away from it.

In order to quantify the trend exhibited in figure 6, we show in figure 7 how the area under the curves shown in the former figure depends on the injection current, for three different values of noise intensity, which can be controlled at will in the numerical model. As we have shown in figure 6, when the injection current increases, the area under the curve increases, reflecting the monotonic decrease in the stochasticity of the coupled-laser system. Interestingly, while increasing the noise intensity, the area under the curve decreases, in general, as could be expected; the decrease is more important far from threshold. This indicates that close to threshold the dynamics is mostly dominated by noise and not by deterministic effects, and thus an increase in the noise level does not influence strongly the statistics of the forbidden patterns.

5. Conclusions

Coupling delays are a natural consequence of the finite speed with which signals travel between interacting dynamical systems. It is important to determine whether the resulting dynamics of this type of system is deterministic or stochastic. Here we have used a recently proposed method to quantify the level of stochasticity of a time series, based on computing the number of forbidden patterns exhibited by the time series, to address this issue in mutually coupled semiconductor lasers. Both the experimental and numerical results presented here show that the leader–laggard dynamics exhibited by this system is stochastic

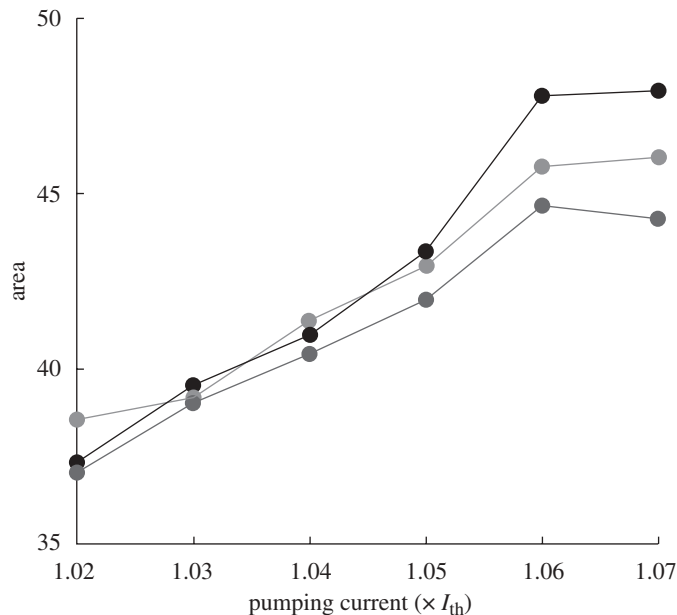


Figure 7. Area under the curves of figure 6 for increasing values of the pump currents (assumed equal for the two lasers). The black line corresponds to a noise intensity of 10^{-15} ps^{-2} , the light grey line to a noise intensity of 10^{-13} ps^{-2} and the dark grey line to a noise intensity of 10^{-11} ps^{-2} .

close to the laser threshold, while the stochasticity is reduced monotonically as the system is pumped further away from threshold. No forbidden patterns are observed for large enough time series in any case, indicating that the deterministic components of the dynamics far from threshold have a high dimensionality.

Financial support has been provided by the Ministerio de Ciencia e Innovación of Spain (project FIS2009-13360 and I3 program) and by the European Commission (GABA project, EC contract 043309).

References

- Ahlers, V., Parlitz, U. & Lauterborn, W. 1998 Hyperchaotic dynamics and synchronization of external-cavity semiconductor lasers. *Phys. Rev. E* **58**, 7208–7213. (doi:10.1103/PhysRevE.58.7208)
- Amigó, J. M., Kocarev, L. & Szczepanski, J. 2006 Order patterns and chaos. *Phys. Lett. A* **355**, 27–31. (doi:10.1016/j.physleta.2006.01.093)
- Amigó, J. M., Zambrano, S. & Sanjuán, M. A. F. 2007 True and false forbidden patterns in deterministic and random dynamics. *Europhys. Lett.* **79**, 50001. (doi:10.1209/0295-5075/79/50001)
- Amigó, J. M., Elizalde, S. & Kennel, M. B. 2008 Forbidden patterns and shift systems. *J. Comb. Theory A* **115**, 485–504. (doi:10.1016/j.jcta.2007.07.004)
- Fischer, I., van Tartwijk, G. H. M., Levine, A. M., Elsässer, W., Göbel, E. & Lenstra, D. 1996 Fast pulsing and chaotic itinerancy with a drift in the coherence collapse of semiconductor lasers. *Phys. Rev. Lett.* **76**, 220–223. (doi:10.1103/PhysRevLett.76.220)
- González, C. M., Torrent, M. C. & García-Ojalvo, J. 2007 Controlling the leader–laggard dynamics in delay-synchronized lasers. *Chaos* **17**, 033122. (doi:10.1063/1.2780131)

- Heil, T., Fischer, I., Elsässer, W., Mulet, J. & Mirasso, C. R. 2001 Chaos synchronization and spontaneous symmetry-breaking in symmetrically delay-coupled semiconductor lasers. *Phys. Rev. Lett.* **86**, 795–798. (doi:10.1103/PhysRevLett.86.795)
- Henry, C. & Kazarinov, R. 1986 Instability of semiconductor lasers due to optical feedback from distant reflectors. *IEEE J. Quantum Electron.* **22**, 294–301. (doi:10.1109/JQE.1986.1072959)
- Herrero, R., Figueras, M., Rius, J., Pi, F. & Orriols, G. 2000 Experimental observation of the amplitude death effect in two coupled nonlinear oscillators. *Phys. Rev. Lett.* **84**, 5312–5315. (doi:10.1103/PhysRevLett.84.5312)
- Hohl, A., van der Linden, H. J. C. & Roy, R. 1995 Determinism and stochasticity of power-dropout events in semiconductor lasers with optical feedback. *Opt. Lett.* **20**, 2396–2398. (doi:10.1364/OL.20.002396)
- Lam, W.-S., Guzdar, P. N. & Roy, R. 2003 Effect of spontaneous emission noise and modulation on semiconductor lasers near threshold with optical feedback. *Int. J. Mod. Phys. B* **17**, 4123–4138. (doi:10.1142/S021797920302209X)
- Mork, J., Tromborg, B. & J. Mark, 1992 Chaos in semiconductor lasers with optical feedback—theory and experiment. *IEEE J. Quantum Electron.* **28**, 93–108. (doi:10.1109/3.119502)
- Ohtsubo, J. 2002 Chaotic dynamics in semiconductor lasers with optical feedback. *Progress in optics*, vol. 44, pp. 1–84. Amsterdam, The Netherlands: Elsevier.
- Sacher, J., Elsässer, W. & Göbel, E. 1989 Intermittency in the coherence collapse of a semiconductor laser with external feedback. *Phys. Rev. Lett.* **63**, 2224–2227. (doi:10.1103/PhysRevLett.63.2224)
- Sano, T. 1994 Antimode dynamics and chaotic itinerancy in the coherence collapse of semiconductor lasers with optical feedback. *Phys. Rev. A* **50**, 2719–2726. (doi:10.1103/PhysRevA.50.2719)
- Takamatsu, A., Fujii, T. & Endo, I. 2000 Time delay effect in a living coupled oscillator system with the plasmodium of *Physarum polycephalum*. *Phys. Rev. Lett.* **85**, 2026–2029. (doi:10.1103/PhysRevLett.85.2026)
- Uchida, A., Rogister, F., García-Ojalvo, J. & Roy, R. 2005 Synchronization and communication with chaotic laser systems. *Progress in optics*, vol. 48, pp. 203–341. Amsterdam, The Netherlands: Elsevier.
- Zanin, M. 2008 Forbidden patterns in financial time series. *Chaos* **18**, 013119. (doi:10.1063/1.2841197)
- Zunino, L., Zanin, M., Tabak, B. M., Perez, D. G. & Rosso, O. A. 2009 Forbidden patterns, permutation entropy and stock market inefficiency. *Physica A, Stat. Mech. Appl.* **388**, 2854–2864. (doi:10.1016/j.physa.2009.03.042)